Mineralogy and Petrology

Ferropericlase inclusions in ultradeep diamonds from Sao Luiz (Brazil): High Li abundances and diverse Li-isotope and trace element compositions suggest an origin from a subduction mélange

--Manuscript Draft--

Manuscript Number:	MIPE-D-17-00187R2
Full Title:	Ferropericlase inclusions in ultradeep diamonds from Sao Luiz (Brazil): High Li abundances and diverse Li-isotope and trace element compositions suggest an origin from a subduction mélange
Article Type:	Supplement Kimberlites
Keywords:	Lithium abundances; lithium isotopes; ferropericlase; diamonds; subduction; serpentinite; carbonates; redox reactions
Corresponding Author:	Gerhard Brey, PhD Goethe-Universitat Frankfurt am Main Frankfurt, GERMANY
Corresponding Author Secondary Information:	
Corresponding Author's Institution:	Goethe-Universitat Frankfurt am Main
Corresponding Author's Secondary Institution:	
First Author:	Hans-Michael Seitz
First Author Secondary Information:	
Order of Authors:	Hans-Michael Seitz
	Gerhard Brey, PhD
	Jeff W. Harris
	Soodabeh Durali-Müller
	Thomas Ludwig
	Heidi Eva Höfer
Order of Authors Secondary Information:	
Manuscript Region of Origin:	GERMANY
Funding Information:	

Ferropericlase inclusions in ultradeep diamonds from Sao Luiz (Brazil): High Li abundances and diverse Li-isotope and trace element compositions suggest an origin from a subduction mélange

Hans-Michael Seitz[1*] • Gerhard P. Brey[1] • Jeffrey W. Harris[2] • Soodabeh Durali-Müller[1] • Thomas Ludwig[3] • Heidi E. Höfer[1]

✉ Gerhard P. Brey
brey@em.uni–frankfurt.de

[1] Institut fuer Geowissenschaften, Mineralogie, Goethe Universitaet Frankfurt, Altenhoeferallee 1, 60438 Frankfurt, Germany

[2] School of Geographical and Earth Sciences, University of Glasgow, Glasgow G12 8QQ, Scotland, UK

[3] Institut fuer Geowissenschaften, Universitaet Heidelberg, Im Neuenheimer Feld 236, 69120 Heidelberg, Germany

Abstract

The most remarkable feature of the inclusion suite in ultradeep alluvial and kimberlitic diamonds from Sao Luiz (Juina area in Brazil) is the enormous range in Mg# [100xMg/(Mg+Fe)] of the ferropericlases (fper). The Mg-richer ferropericlases are from the

boundary to the lower mantle or from the lower mantle itself when they coexist with ringwoodite or Mg- perovskite (bridgemanite). This, however, is not an explanation for the more Fe-rich members and a lowermost mantle or a "D" layer origin has been proposed for them. Such a suggested ultra-deep origin separates the Fe-rich fper-bearing diamonds from the rest of the Sao Luiz ultradeep diamond inclusion suite, which also contains Ca-rich phases. These are now thought to have an origin in the uppermost lower mantle and in the transition zone and to belong either to a peridotitic or mafic (subducted oceanic crust) protolith lithology. We analysed a new set of more Fe-rich ferropericlase inclusions from 10 Sao Luiz ultradeep alluvial diamonds for their Li isotope composition by solution MC-ICP-MS (multi collector inductively coupled plasma mass spectrometry), their major and minor elements by EPMA (electron probe micro-analyser) and their Li-contents by SIMS (secondary ion mass spectrometry), with the aim to understand the origin of the ferropericlase protoliths. Our new data confirm the wide range of ferropericlase Mg# that were reported before and augment the known lack of correlation between major and minor elements. Four pooled ferropericlase inclusions from four diamonds provided sufficient material to determine for the first time their Li isotope composition, which ranges from δ^7Li +9.6 ‰ to -3.9 ‰. This wide Li isotopic range encompasses that of serpentinized ocean floor peridotites including rodingites and ophicarbonates, fresh and altered MORB (mid ocean ridge basalt), seafloor sediments and of eclogites. This large range in Li isotopic composition, up to 5 times higher than 'primitive upper mantle' Li-abundances, and an extremely large and incoherent range in Mg# and Cr, Ni, Mn, Na contents in the ferropericlase inclusions suggests that their protoliths were members of the above lithologies. This mélange of altered rocks originally contained a variety of carbonates (calcite, magnesite, dolomite, siderite) and brucite as the secondary products in veins and as patches and Ca-rich members like rodingites and ophicarbonates. Dehydration and redox reactions during or after deep subduction into the transition zone and the upper parts of the lower mantle led to the formation of diamond and ferropericlase

inclusions with variable compositions and a predominance of the Ca-rich, high-pressure silicate inclusions. We suggest that the latter originated from peridotites, mafic rocks and sedimentary rocks as redox products between calcite and SiO_2.

Keywords Lithium isotopes • Ferropericlase • Diamond • Subduction • Serpentinite • Redox reactions

Introduction

Inclusions in alluvial diamonds from Sao Luiz (Juina area) in Brazil provided the first comprehensive evidence for an origin of diamonds from the upper parts of the lower mantle (Harte and Harris 1994). These authors reported coexisting ferropericlase and Mg-perovskite (bridgmanite), which is the stable mineral paragenesis of a lherzolithic mantle below the 670 km discontinuity. More localities of ultradeep diamonds have been found since and Harte (2010) gave a comprehensive overview of these and the earlier findings.

The Mg# of coexisting Mg-perovskite and fper from the lower mantle or the upper/lower mantle boundary region are about 90 and 76, respectively, for a primitive Earth mantle (see Fig. 1 in the electronic appendix) with corresponding shifts to higher and lower values for depleted or more Fe-rich mantle according to the partition coefficients taken from Frost and Langenhorst (2002). The range of Mg# for Mg-perovskites from Sao Luiz diamonds lies between 94 and 86 (Fig. 1); the corresponding ferropericlases have a range between 85 and 55. A number of ferropericlases in this compositional range coexist with Ca-perovskite or TAPP (Jeffbenite; a tetragonal high pressure garnet) or olivine (presumably former ringwoodite), which shows that the whole mineral paragenesis from the upper/lower mantle boundary and the uppermost lower mantle is present in Sao Luiz diamond mineral inclusions

(Hayman et al. 2005; Kaminsky et al. 2009; Kaminsky et al. 2001). Compared to the total number of inclusions in diamonds, the lower mantle paragenesis is rare (Fig. 1). However, a large proportion of the ferropericlases have Mg# too low for a peridotitic composition and range down to 35 (see Fig. 1; Harte et al. 1999; Hayman et al. 2005; Hutchinson et al. 2001; Kaminsky et al. 2001). A number of ferropericlases also have very high Mg# up to 89 that could occur in ultra-depleted peridotite. However, Mg-perovskite inclusions with correspondingly highest Mg# were never reported.

The range in Mg# led Harte et al. (1999) and Hayman et al. (2005) to suggest that the origin of the diamonds with the more Fe-rich ferropericlases was in the D" layer or the lowermost mantle. An alternative idea by (Liu 2002) proposed a redox precipitation of diamond and ferropericlase from ferromagnesites in the lower mantle. However, such reactions can occur at any depth in the diamond stability field and are not restricted to the lower mantle. Brey et al. (2004) interpreted the ferropericlases as high-pressure/temperature phases derived from Fe-rich hybrid lithologies of peridotite mixed with subducted eclogite/sediment in the upper mantle or transition zone.

Harte (2010) and Harte and Hudson (2013) concluded for the lower mantle mineral assemblage with the more Mg-rich ferropericlases that the greatest depth for diamond formation is about 100 km below the transition zone – lower mantle boundary. This conclusion is based on the pressure - temperature constraints coming from the Al-bearing Mg-Si perovskites, which co-exist with some ferropericlases and on Schreinemaker analysis. Harte (2010) and Harte and Richardson (2012) concluded that the protoliths of the diamond inclusions are meta-peridotites, subducted meta-basites and sedimentary material for the Ca-rich inclusion suite and associated uncommon mineral inclusions and possibly "special bulk compositions" for the more Fe-rich ferropericlases. Evidence for crustal recycling comes from carbon isotope ratios of diamonds and oxygen isotope ratios of their inclusions (Zedgenizov et al. 2014; Thomson et al. 2014 and Burnham et al. 2015). Walter et al. (2008) and Thomson et

al. (2016) explained the Ca-silicates as precipitates from percolating primary carbonatitic melts and Walter et al. (2011) supply evidence that mafic crustal material was subducted into the upper portions of the lower mantle. Extremely high Li concentrations in ferropericlase inclusions from Sao Luiz diamonds (up to ~24 μg/g) and Kankan, Guinea (up to ~50 μg/g were previously reported (Kaminsky et al. 2001; Seitz et al. 2003). From mass balance considerations Seitz et al. (2003) estimated that the source region of the Kankan diamonds in the lower mantle contained several times higher lithium abundances than the primitive upper mantle (Eggins et al. 1998; Jagoutz et al. 1979; McDonough and Sun 1995; Seitz and Woodland 2000).

In this work we explore possible protoliths for the more Fe-rich ferropericlase inclusions in ultradeep diamonds more closely through a study of their trace elements (Na, Mn, Ni) as well as lithium abundances and isotopes. Inclusions in diamonds are notoriously small but lithium was found to occur generally in high concentrations in the ferropericlase inclusions (Seitz et al. 2003) that are sufficient to allow the determination of the Li isotopic composition by solution MC-ICP-MS for the first time. Li-isotopes have the potential to constrain the rock types and help to identify subducted material because of the tremendous fractionation of the Li-isotopes during near surface processes.

Sample preparation and analytical methods

Ferropericlase inclusions were released from ten diamonds (BZ300 - BZ309) in a sealed stainless steel crusher using the technique described by Harris and Gurney (1979). Of the ten diamonds, four contained single and six contained multiple inclusions (Table 1). The single inclusions, a pair from one and three from another diamond were not large enough and their

Li-contents were too low for isotopic analysis; they were used for EPMA measurements and the analysis of the Li-content by SIMS. In addition to these, one grain each from the remaining 4 diamonds with multiple inclusions were mounted in araldite within small brass cylinders (2.6 mm in diameter). In all, 13 ferropericlase inclusions from the ten diamonds were polished and analysed by EPMA and ion microprobe. Sixteen grains remained from the 4 diamonds with multiple inclusions. These were pooled for each individual diamond to determine the Li isotopic composition by solution MC-ICP-MS.

Major elements were analysed with a JEOL JXA-8900 RL electron microprobe. The Li contents were determined with a modified CAMECA 3f-IMS ion microprobe (SIMS) using a $^{16}O^-$ primary beam with a diameter of ~10 μm. Estimated precision and accuracy is better than ±20 % at the μg/g level. Because of the small size of the inclusions, only 1 to 2 spots could be analysed per grain.

Li isotopes were analyzed from solution by MC-ICP-MS (Neptune, Thermo Scientific). Digestion of the ferropericlase composites (0.06 to 0.11 mg) and column separation was based on the procedure of Seitz et al. (2004). In order to reduce the chemistry blank as much as possible, we minimized the amount of acids needed for the dissolution. We further refined the procedure and reduced it to a 3-step dissolution: i) 0.25 ml 6M HNO_3 and 0.25 ml conc. HF; ii) 0.5 ml 6M HCl; iii) 0.5 ml 6M HNO_3. Column separation was carried out with 0.18 ml 5M HNO_3 and 0.72 ml 100% methanol.

Prior to chromatography of the ferropericlase solutions**,** columns were calibrated using solutions with different MgO and FeO contents. Solutions containing 45 wt% MgO/55 wt% FeO and 75 wt% MgO/25 wt% FeO were doped with 25 ng/g Li. Chromatography was tested using MgO-FeO matrices doped with only 2.5 ng/g Li (L-SVEC). With the collection of 10 ml of the eluate, all lithium was recovered and no isotope fractionation was detected (Fig. 2 of the electronic appendix). Solutions were run through a Cetac Aridus® nebulizer fitted with a PFA spray chamber and an ESI microconcentric nebulizer with an uptake rate of 20 μl/min.

With standard H-cones an intensity of 40-50 pA, (10^{11} Ω resistor, 4-5 V) for ^{7}Li at a 10 ng/g concentration level is achieved. In order to monitor dissolution and column chemistry, we processed JB-2 basalt reference material, along with the ferropericlase samples, at high and low concentration level (1 ng/g). To achieve a higher Li concentration in the analytical solutions, samples were taken up in only 0.2 ml 2 % $HN0_3$. This, and the use of a 20 µl/min nebulizer, made three to four consecutive measurements possible. The chemistry was performed in two separate sets. In the first 'run', sample BZ 300 was processed along with a standard and a chemical blank. This resulted in successful determination of the Li isotope composition of BZ 300. Subsequently, samples BZ 301, BZ 305, BZ 309, a second standard and a chemical blank were processed in a consecutive session. The chemical blanks, run along with the samples and diluted in the same manner, were used for correction. The limit of blank ($LoB = mean_{(blank)} + 3\times SD$) for the two analytical sessions was about 32 pg/g - based on repeated measurements of wash solutions (2% HNO_3). The limit of detection ($LoD = LoB_{(blank)} + 3(SD_{low\ concentration\ sample\ BZ\ 301})$) is 38 pg. Sample and chemical blank signals are well above LoD. In the first analytical session, the intensity on ^{7}Li for BZ 300 was 305 mV, corresponding to 850 pg. The contribution to this signal by the chemical blank is 195 pg/g. By subtracting the chemical blank signal from that of the fper sample the real isotopic value was calculated. Repeated measurement of this sample in the second analytical campaign, along with the other three fper samples, gave identical results. Intensities and isotopic compositions of the two different chemical blanks were also identical, and Li concentrations of the sample solutions were well above LoD (390 pg for BZ 301; 1240 pg for BZ 305 and 400 pg for BZ 309). Sample analysis was carried out sequentially by 'bracketing' the sample with the L-SVEC standard (Flesch et al., 1973). Isotope compositions are expressed as per mil deviations from the NIST L-SVEC standard: $\delta^{7}Li = [(^{7}Li/^{6}Li)_{sample}/(^{7}Li/^{6}Li)_{L\text{-}SVEC\ standard}-1]*1000$. Internal precision is typically between 0.2–0.6 ‰ (2SE) and long term reproducibility, determined on replicate dissolutions over the last 4 years of the geological standard JB-2 (δ^{7}Li

+5.1 ‰) is about 1.2 ‰ (2σ). The 1 ng/g JB2 solution and the 2.5 ng/g 'MgO/FeO L-SVEC test solution' (see above), measured together with the samples, gave δ^7Li +4.9 ‰ ±0.5 (2σ) and δ^7Li +0.2 ‰ ±0.4 ‰ (2σ), respectively.

Results

Our new data on major and trace elements augment and complement the existing data set on ferropericlases from Sao Luiz diamonds (Harte et al. 1999; Hayman et al. 2005; Hutchinson et al. 2001; Kaminsky et al. 2001). The present sample set confirms the most remarkable feature of the inclusion suite, the extreme range in Mg#, with new values between 82.6 and 59.8 (Table 2 and Fig. 2). The literature data set combined with our new data shows an overall range of Mg# from 35 to 87. As described by previous workers (Harte et al. 1999; Hayman et al. 2005) ferropericlases with Mg# >55 are homogeneous from rim to rim, while those with Mg# < 55 show spotty exsolutions of magnesioferrite (Figs. 3 and 4 in the electronic appendix)**.** Minor elements within our ferropericlases are also very variable with NiO and Cr_2O_3 ranging from 0.2 – 1.1 wt % and 0.04 – 0.44 wt % respectively. Li contents are 2 - 44 µg/g. Na_2O varies from close to zero to 1.4 wt %, with MnO being equally low, almost zero to 1.5 wt %. Figure 2 shows the range of the minor elements Li, Na, Ni and Mn. It can be seen, that ferropericlases with low and high Mg# have both low and high minor element contents without any correlation. Most noticeable is the fact that the ferropericlases with the highest Mg# (which should correspond to a peridotitic lithology) have very low NiO and high MnO contents, far too low and too high, respectively, for a peridotitic mantle (Fig. 2 c, d). On the other hand, ferropericlases with low Mg#, which are not linked with a peridotite lithology, have high NiO contents.

Previously, Kaminsky et al. (2001 and 2009) determined Li-concentrations in ferropericlases by LA-ICP-MS (laser ablation multi collector inductively coupled plasma mass spectrometry). These data together with our newly measured Li concentrations by SIMS are presented in Table 2 and shown in Fig. 2. Two inclusions (BZ 302 and BZ 308) with Mg# ~ 71 have the highest Li concentrations (37 and 44 μg/g, respectively) reported so far for inclusions in diamonds from Sao Luiz. These Li values are in the same range as the two high Mg#-ferropericlases (Mg#~86) from Kankan (Guinea; see Fig. 2a). The two inclusions from diamond BZ 307 have identical Mg# and similar Li-contents (4.7 and 6.8 μg/g), but whilst the three ferropericlases from diamond BZ 306 (Fig. 2a) have similar Mg#, one contains only 4.3 μg/g Li and the other two 13.9 and 14.7 μg/g. Taken together with the Li abundances determined by Kaminsky et al. (2001) the Li contents in ferropericlases from Sao Luiz diamonds mostly fall within the range of 2 to 23 μg/g with no correlation with their Mg#.

The four pooled ferropericlase composites from diamonds BZ 300, 301, 305 and 309 have Li isotope compositions (δ^7Li) of +9.6, + 2.1, + 0.3 and -3.9 ‰, respectively (Table 1 and Fig. 3). We had selected one grain from each of the diamonds to determine their chemical composition. If this is taken as representative for the whole composite then there is no correlation with either Li abundances (Fig. 3) nor with Mg# (given in Table 2). The heaviest δ^7Li value of +9.6 ‰ was identified for the sample with the lowest Li content (2.4 μg/g), whilst the lightest δ^7Li value of -3.9 ‰ is in the sample with a Li abundance of 5.9 μg/g. In theory, each individual inclusion could be different in chemical and isotopic composition and, indeed, we found one diamond with 3 fper inclusions of identical Mg# but differing Li contents (BZ 306). In the light of the incoherency of all other chemical parameters, it appears highly unlikely that a coherency would arise for the chemical parameters of these individual inclusions. It remains a fact that the Li-isotopes and all other chemical parameters form a cloud showing no correlations, which is only typical for a melange of rock types.

Discussion and conclusions

Growth of ferropericlase inclusions in subduction-modified lower mantle peridotite

The large variability in the chemical composition of ferropericlase inclusions from Sao Luiz diamonds indicates significant heterogeneities and different physical and chemical conditions in the deep mantle at the time of diamond formation. In particular the Fe-rich nature of the ferropericlases is prominent in this suite. Only a fper inclusion in BZ 305 diamond is close to that of fper from a primitive peridotitic mantle in Mg# and Ni and Mn contents (Fig. 2). . Its Li content is 31.5 μg/g. Assuming that the primitive lower mantle consists of 20 % ferropericlase (with the measured 31.5 μg/g Li), 75 % Mg-perovskite (with 0.1 μg/g Li) and 5 % Ca-perovskite (with 2.5 μg/g Li taken from Kaminsky et al., 2001), we calculate a bulk composition with 6.5 μg/g Li. The Li concentration estimated here for a primitive lower mantle is 4 to 5 times higher than in the upper mantle, (see estimates by Eggins et al. 1998; Jagoutz et al. 1979; McDonough and Sun 1995; Seitz and Woodland 2000). Therefore, Li must have been introduced into the source region of LM diamond formation and a viable process is via subduction of serpentinites, altered oceanic crust and terrigenous sediments.

Origin of Fe-rich ferropericlase inclusions from the D" layer or as exsolutions from a post-perovskite phase?

To invoke an origin of the more Fe-rich ferropericlases from the lowermost mantle or the D" layer, one would have to explain why these parts of the mantle are so tremendously heterogeneous, not only in Mg#, but also in trace elements and in mineralogy (ferropericlases can occur in the same diamond with SiO_2, or Mn-rich ilmenite or spinel (Kaminsky et al. 2001). It can be seen in Fig. 2 that there is no systematic relationship between ferropericlase Mg# and trace element abundances like Li, Na_2O, Ni and Mn, nor amongst the latter elements. If the range of Mg#'s of the ferropericlases originated from preferential partitioning of Fe from the post perovskite phase into ferropericlase in the lower mantle, as suggested by Hayman et al. (2005), or from contamination of the Earth's core material in the D" layer (Harte et al. 1999 and Wirth et al. 2014), one could expect a more systematic partitioning behaviour of these elements relative to each other, with certainty for Ni an Mn with Mg#. Low pressure phases like Mn-rich ilmenites and spinels coexisting with ferropericlase and the lack of correlation of chemical parameters within the ferropericlases refute an origin in the lowermost mantle or the D" layer. Also, these parts of the mantle would have to be highly diversified in their Li-isotope ratios because our measurements give δ^7Li between +10 and -4 ‰.

A hybrid origin of Fe-rich ferropericlase inclusions?

Brey et al. (2004) suggested a "hybrid" model where Fe-rich ferropericlases grow from peridotite + subducted eclogite/sediment mixtures at transition zone pressures by the reaction "ringwoodite = ferropericlase + SiO_2" (see three phase field in Fig. 1 in the Appendix). Such a model could potentially explain the non-coherency of chemical parameters and the variability of δ^7Li in the ferropericlase inclusions, However, Fe-rich "ringwoodites" have not yet been identified so far in Sao Luiz diamonds. Mg-values of known "ringwoodite" compositions of inclusions in diamonds range from 87 to 89 (Kaminsky et al., 2001), and are

far too Mg-rich to coexist with Fe-rich ferropericlases. Similarly, Fe-rich ferropericlases together with a SiO_2 phase have not been described yet from Sao Luiz.

The large variability of δ^7Li in ferropericlase inclusions - possible causes

The non-correlation between Mg# and trace element compositions within the ferropericlases of Sao Luiz diamonds extends to the Li-isotopes, which range between about δ^7Li +10 and -4 ‰. These results indicate an extreme diverse chemical composition for the diamond protoliths or, less likely, kinetic isotope disequilibria processes.

Large inter-mineral Li-isotope disequilibria are observed in mantle xenoliths. Ionov and Seitz (2008) found that the magnitude of this isotopic fractionation is a function of the cooling rate upon eruption. Other work (Aulbach et al. 2008; Aulbach and Rudnick 2009; Yacob et al. 2012) did not find such a dependency. It was, however, found that the Li isotope disequilibria are associated, in many cases with the addition of Li to peridotite (e.g. Rudnick and Ionov 2007). In general, element diffusivities decrease strongly with pressure in silicates and may even stagnate at pressures reaching the transition zone (e.g. Van Orman et al. 2001). The diffusivity of Fe-Mg in olivine at 15 GPa and 1500 °C, for example, becomes extremely slow and is orders of magnitude slower than under upper mantle conditions (e.g. Dohmen et al. 2007; Holzapfel et al. 2009). We can only speculate on Li diffusion in ferropericlase under such high P/T conditions but assuming that Li diffusivity in lower upper to upper lower mantle phases is extremely slow, kinetic Li isotope fractionation would likely play, if at all, a very minor role only.

Rather we suggest that the Li-isotope compositions observed in the studied suite of ferropericlase inclusions likely reflect originally low pressure lithologies. The δ^7Li values of the ferropericlases between + 10 and -4 ‰ are in the range of serpentinites, marine sediments and eclogites and we equate them to these rock types (Fig. 3). The analysis of modern day

serpentinites from the ocean floor shows that serpentinisation diversifies the δ^7Li of ~ +3.2 ‰ of a primitive mantle to a range between -12 to +14‰ (Fig. 3; references given in the figure caption). This range originates through a differing Li-isotope partitioning behaviour between alteration fluids and the various serpentine minerals. The partitioning between fluids and serpentine minerals is such that it favours heavy δ^7Li values in chrysotile and light δ^7Li values in lizardite or antigorite (Wunder et al., 2010). Low temperature processes in general lead to a high variability and diversification of the Li-isotopes and to an addition of Li like in altered MORB and marine sediments (Fig. 3). Eclogites mostly show negative δ^7Li values with a wide range in Li-contents (diamonds in Fig. 3). Even though a small overlap occurs, processes leading to eclogitization fractionate the Li-isotopes further compared to altered MORB (Marschall et al., 2007). This may occur at the very early metamorphic stages at low temperatures. Low temperature altered lithologies from a subduction mélange are therefore suitable protoliths from which diamonds and ferropericlases with their wide variation of δ^7Li and Li contents grew. In contrast, the carbon isotope ratios of the diamonds with ferropericlase inclusions from Sao Luiz have a restricted range of δ^{13}C between -2.1 and -7.7 ‰ around the mantle value (Zedgenizov et al., 2014) and in a similar range of lower mantle diamonds from Kankan (δ^{13}C = -0.5 to -6.6 ‰; Stachel et al. 2002). The total range of δ^{13}C values for Sao Luiz diamonds is from +2.7 to -25.3 ‰. In a comprehensive study, Stachel et al. (2009) confirmed the general difference in the distribution of δ^{13}C between the various inclusion parageneses, especially eclogitic versus peridotitic. However, they also demonstrated that there are no significant correlations between the major element compositions of the inclusions and the carbon isotope composition of the diamonds, i.e. the diamond forming melts or fluids are introduced externally into the substrate (e.g. Haggerty 1986; Stachel and Harris 1997; Walter et al. 2008). There is also no correlation of fper major and minor element abundances with the carbon isotope composition of their host diamonds

including Na_2O (Stachel, pers. communication). Li as an alkali metal also belongs to the substrate and a correlation of its isotope ratios with $\delta^{13}C$ of the diamonds is not to be expected.

A model for the origin of Fe-rich ferropericlase inclusions in diamonds

Oceanic lithosphere is just a diverse reservoir consisting of clay, carbonate and siliceous sediments, basalts, gabbros, cumulates and harzburgite, augmented by continental derived sediments at active continental margins. Further diversification to this rock pile occurs by low and high temperature alteration and associated mass transport processes. Serpentinization is an especially effective process to form local inhomogeneities. Magnesite, ankerite, siderite, brucite, magnetite and sometimes native iron may be formed locally in pods and veins. It thus produces local low temperature domains with an extreme variability of FeO/MgO ratios. The formation of Ca-rich lithologies like rodingites and ophicarbonates are also connected with serpentinization. These rock types are a priori not periclase-bearing but they are sensitive to oxidation/reduction to diamond+ferropericlase and diamond+Ca-silicate assemblages by redox reactions such as

(1) $MgCO_3 + CH_4 = MgO + 2C_{(diamond)} + 2\ H_2O$

(2) $MgCO_3 + Fe = 2(Mg_{0.5}Fe_{0.5})O + C_{(diamond)} + ½\ O_2$ (in the presence of metallic Fe-Ni)

(3) $2MgCO_3 + FeS + Fe_3O_4 = 6(Mg_{0.33}Fe_{0.67})O + 2C_{(diamond)} + SO_2 + 3O_2$

(in the presence of sulphide and magnetite)

(4) $SiO_2 + CaCO_3 = CaSiO_3 + C_{(diamond)} + O_2$

Highly variable iron oxidation states in ferropericlase inclusions from Brasilian and Australian diamond localities were determined by Longo et al. (2009) with the flank method

(Höfer and Brey 2007). The ensuing range of oxygen fugacities probably includes that of the above redox reactions. The ferropericlases are the redox products mostly of carbonates during diamond formation (e.g. reactions 1-3 above). Those ferropericlases with the highest Mg# and low Ni and high Mn could be derived from former magnesites and those with the lowest Mg# from magnesium rich ankerites. Intermediate Mg# ferropericlases with both high and low Ni and Mn, will be redox products of Mg-richer carbonates or more complex diamond forming redox reactions in the presence of Fe, sulphides and magnetite. Ferropericlases with high Mg# and also high Ni are of peridotitic origin and have their lower mantle counterpart in the Mg-Si-perovskites.

Another prominent feature of the Sao Luiz diamond inclusion suite seems to be an over-abundance of Ca-phases (Harte 2010; Hayman et al. 2005). These are $CaSiO_3$ (presumably former perovskite, but probably also primary walstromite); larnite (ß-Ca_2SiO_4), perovskite ($CaTiO_3$, where Ti is replaced by Si to various extents), merwinite ($Ca_3Mg(SiO_4)_2$ + walstromite-structured $CaSiO_3$ + olivine (Zedgenizov et al., 2014), $CaCO_3$ and dolomite (Brenker et al. 2007; Harte et al. 1999; Hayman et al. 2005; Hutchinson et al. 2001; Kaminsky et al. 2001). Some of the phases and phase assemblies like merwinite+olivine or Ti-bearing Ca-perovskites are not stable in the lower mantle but at shallower depths. Also, larnite and $CaSi_2O_5$ as separate inclusions in a single diamond exclude an origin from the lower mantle because this paragenesis is stable only in the transition zone (Gasparik, 1994). A contacting pair in an inclusion may, however, be exsolved Ca-perovskite from the lower mantle (Joswig et al., 1999). The common occurrence of Ca-phases and especially Eu-anomalies in Ca-perovskites led Harte et al. (1999) to suggest that parts of the protoliths were altered basalts and their sedimentary cover. Also, the common occurrence of Ca-perovskites is not matched either by a corresponding abundance of Mg-Si-perovskites (if they belong to the peridotitic suite) nor of majoritic garnets (if the Ca-silicates belong to an eclogitic suite). Their abundance may, however, be increased by diamond forming reactions like (4) (see above),

where the precursor material may be marly limestones, ophicarbonates or rodingites. Other inclusion phases identified from Sao Luiz diamonds are magnetite, ilmenite with up to 11.5 wt% MnO, Cr-Ti spinel and SiO_2, with rarer phases of CaTi-perovskite, sphene, rutile, corundum and native Fe and Ni (Harte 2010). All these phases do occur in altered oceanic floor lithologies and sediments and are further evidence that the diamond inclusion suite from Sao Luiz is derived from a subducted ophiolite melange. There seems to be now a general acceptance that diamonds grow by redox reactions from the interaction of reduced/oxidized fluids or melts with oxidized/reduced protoliths. If uprising, methane-rich fluids interact with the subducted melange with its carbonated material, they would react to form diamonds and a water rich fluid, produced either by reduction of carbonates or by oxidation of methane (Green et al. 1987; Taylor and Green 1987). As shown by Bulanova et al. (2010) for ultradeep diamonds from Collier-4 kimberlites (within the Sao Luiz area), diamond formation occurred in several stages and from differing sources. A U-Pb age of 101 Ma was determined by LA-ICP-MS from a CaTiSi-perovskite; this age is close to the kimberlite emplacement age of about 93 Ma and expresses only the youngest age of diamond formation (Bulanova et al., 2010). These authors and Harte and Richardson (2012) in more detail provided a model, where diamonds grow in a subducting slab and in the uppermost lower mantle in Mesozoic times.

Acknowledgements We profited from discussions with Thomas Stachel, Alan Woodland, Sonja Aulbach, and Andrei Girnis. David Green made valuable suggestions to the manuscript. We thank Anna Karina Neumann, Thomas Kautz, Franz Kneissl and Jan Heliosch for technical advice and assistance. We also thank the reviewers Ben Harte and Galina Bulanova and the editor, Roberta Rudnick, for constructive comments on the manuscript. Co-author J.W.H. thanks the Diamond Trading Company (a member of the DeBeers Group of

Companies) for the donation of the diamonds used in this study. This study was financially supported by the Deutsche Forschungsgemeinschaft through grant BR 1012/24-1 to G.B.

References

Aulbach S, Rudnick RL, McDonough WF (2008) Li-Sr-Nd isotope signatures of the plume and cratonic lithospheric mantle beneath the margin of the rifted Tanzanian craton (Labait) Contrib Mineral Petr 155:79-92

Aulbach S, Rudnick RL (2009) Origins of non-equilibrium lithium isotopic fractionation in xenolithic peridotite minerals: Examples from Tanzania. Chem Geol 258:17-27

Burnham AD, Thomson AR, Bulanova GP, Kohn SC, Smith CB, Walter MJ (2015) Stable isotope evidence for crustal recycling as recorded by superdeep diamonds. Earth Planet Sc Lett 432:374–380

Benton LD, Ryan JG, Savov IP (2004) Lithium abundance and isotope systematics of forearc serpentinites, Conical Seamount, Mariana forearc: Insights into the mechanics of slab-mantle exchange during subduction. Geochem Geophys Geosy 5, issue 8, Q08J12

Bouman C, Elliott T, Vroon PZ (2004) Lithium inputs to subduction zones. Chem Geol 212:59-79

Brenker FE, Vollmer C, Vincze L, Vekemans B, Szymanski A, Janssens K, Szaloki I, Nasdala LWJ, Kaminsky F (2007) Carbonates from the lower part of transition zone or even the lower mantle. Earth Planet Sc Lett 260:1-9

Brey GP, Bulatov V, Girnis A, Harris JW, Stachel T (2004) Ferropericlase - a lower mantle phase in the upper mantle. Lithos 77:655-663

Bulanova GP, Walter MJ, Smith CB, Kohn SC, Armstrong LS, Blundy J, Gobbo L (2010). Mineral inclusions in sublithospheric diamonds from Collier 4 kimberlite pipe, Juina,

Brazil: subducted protoliths, carbonated melts and primary kimberlite magmatism. Contrib Mineral Petr 160:4, 489-510

Chan L-H, Alt JC, Teagle DAH (2002) Lithium and lithium isotope profiles through the upper oceanic crust: a study of seawater-basalt exchange at ODP Sites 504B and 896A. Earth Planet Sc Lett 201:187-201

Chan L-H, Leeman WP, Plank T (2006) Lithium isotopic composition of marine sediments. Geochem Geophys Geosy 7 Nr. 6:1-25

Chan LH, Edmond JM, Thompson G, Gillis K (1992) Lithium isotopic composition of submarine basalts: implications for the lithium cycle in the oceans. Earth Planet Sc Lett 108:151-160

Decitre S, Deloule E, Reisberg L, James R, Agrinier P, Mevel C (2002) Behaviour of Li and its isotopes during serpentinisation of oceanic peridotites. Geochem Geophys Geosy 3:1-20

Dohmen, R., Becker, H.-W., Chakraborty, S., 2007. Fe – Mg diffusion in olivine I : experimental determination between 700 and 1 , 200 ° C as a function of composition , crystal orientation and oxygen fugacity. Phys Chem Miner 34:389-407

Eggins SM, Rudnick RL, McDonough WF (1998) The composition of peridotites and their minerals: a laser-ablation ICP-MS study. Earth Planet Sc Lett 154:53-71

Flesch G, Anderson AR, Svec HJ (1973) A secondary isotopic standard for $^{6}Li/^{7}Li$ determinations. Int J Mass Spectrom 12:265-272

Frost DJ, Langenhorst F (2002) The effect of Al_2O_3 on Fe-Mg partitioning between magnesiowüstite and magnesium silicate perovskite. Earth Planet Sc Lett 199:227-241

Frost DJ, Langenhorst F, van Aken PA (2001) Fe-Mg partitioning between ringwoodite and magnesiowüstite and the effect of pressure, temperature and oxygen fugacity. Phys Chem Miner 28:455-470

Gasparik T (1994) A petrogenetic grid for the system MgO-Al_2O_3-SiO_2. J Geol 102:97-109

459 Green DH, Falloon TJ, Taylor WR (1987) Mantle-derived magmas - roles of variable source
460 peridotite and variable C-H-O fluid compositions, in: Mysen BO (ed) Magmatic
461 processes: Physicochemical principles. The Geochemical Society, London, pp. 139-
462 154
463 Haggerty SE (1986) Diamond genesis in a multiply-constrained model. Nature 320, 34-38
464 Harris J.W, Gurney JJ (1979) Inclusions in diamond. In: Field JE (ed) The properties of
465 diamond, 555-591
466 Harte B (2010) Diamond formation in the deep mantle: the record of mineral inclusions and
467 their distribution in relationship to mantle dehydration zones. Mineral Mag 74:189-
468 215
469 Harte B, Harris JW (1994) Lower mantle association preserved in diamonds. Mineral Mag
470 58A:384-385
471 Harte B, Harris JW, Hutchinson MT, Watt GR, Wilding MC (1999) Lower mantle mineral
472 associations in diamonds from Sao Luiz, Brazil. In: Fei Y, Bertka C, Mysen BO (eds)
473 The J.B. Dawson Volume, Proceedings of the VIIth International Kimberlite
474 Conference. Red Roof Design, Capetown, 372--382
475 Harte B, Richardson S (2012) Mineral inclusions in diamonds track the evolution of a
476 Mesozoic subducted slab beneath West Gondwanaland. Gondwana Res 21:236–245
477 Harte B, Hudson N (2013) Mineral associations in diamonds from the lowermost upper
478 mantle and uppermost lower mantle. Proc 10th Int Kimb Conf, 235-253
479 Hayman PC, Kopylova MG, Kaminsky FV (2005) Lower mantle diamonds from Rio Soriso
480 (Juina area, Mato Grosso, Brazil). Contrib Mineral Petr 149:430-445
481 Holzapfel C, Chakraborty S, Rubie DC, Frost DJ (2009) Fe-Mg interdiffusion in wadsleyite:
482 The role of pressure, temperature and composition and the magnitude of jump in
483 diffusion rates at the 410 km discontinuity. Phys Earth Planet In 172(1-2):28-33

Höfer HE, Brey GP (2007) The iron oxidation state of garnet by electron microprobe: Its determination with the flank method combined with major-element analysis. Am Mineral 92:873-885

Hutchinson MT, Hursthouse MB, Light ME (2001) Mineral inclusions in diamonds: associations and chemical distinctions around the 670-km discontinuity. Contrib Mineral Petr 142:119-126

Ionov D, Seitz H-M (2008) Lithium abundances and isotopic compositions in mantle xenoliths from subduction and intra-plate settings: Mantle sources vs. eruption histories. Earth Planet Sc Lett 266(3-4):316-331

Jagoutz E, Palme H, Baddenhausen H, Blum K, Cendales M, Dreibus G, Spettel B, Lorenz V, Wänke H (1979) The abundances of major, minor and trace elements in the Earth´s mantle as derived from primitive ultramafic nodules. Proc Lunar Planet Sci Conf 10th, 2031-2050

Joswig W, Stachel T, Harris JW, Baur WH, Brey GP (1999) New Ca-silicate inclusions in diamonds —tracers from the lower mantle. Earth Planet Sc Lett 173:1-6

Kaminsky FV, Khachatryan GK, Andreazza P, Araujo D, Griffin WL (2009) Super-deep diamonds from kimberlites in the Juina area, Mato Grosso State, Brazil. Lithos 112S:833-842

Kaminsky FV, Zakharchenko OD, Davis R, Griffin WL, Khachatryan-Blinova GK, Shiryaev AA (2001) Superdeep diamonds from the Juina area, Mato Grosso State, Brazil. Contrib Mineral Petr 140:734-753

Liu L (2002) An alternative interpretation of lower mantle mineral associations in diamonds. Contrib Mineral Petr 144:16-21

Longo M, McCammon C, Bulanova G, Kaminsky FV, Tappert R (2009) Oxygen fugacity determined from iron oxide state in natural (Mg,Fe)O ferropericlase: new insights for lower mantle diamond formation. EOS Trans. AGU 90(52), DI23A-1675

510 Marschall HR, Pogge von Strandmann, PAE, Seitz H-M, Elliott T, Niu Y (2007) The lithium
511 isotopic composition of orogenic eclogites and deep subducted slabs. Earth Planet Sc
512 Lett 262:563–580
513 Marschall HR, Wanless VD, Shimizu N, Von Strandmann PAE, Elliott T, Monteleone B
514 (2017) The boron and lithium isotopic composition of mid-ocean ridge basalts and the
515 mantle. Geochim Cosmochim Ac, 207:102-138
516 McDonough WF, Sun S-S, 1995. The composition of the Earth. Chem Geol 120:223-253.
517 Rudnick RL, Ionov DA (2007) Lithium elemental and isotopic disequilibrium in minerals
518 from peridotite xenoliths from far-east Russia: Product of recent melt/fluid–rock
519 reaction. Earth Planet Sc Lett 256:278-293
520 Seitz H-M, Brey GP, Lahaye Y, Durali S, Weyer S (2004) Lithium isotopic signatures of
521 peridotite xenoliths and isotopic fractionation at high temperature between olivine and
522 pyroxenes. Chem Geol 212:163-177
523 Seitz H-M, Brey GP, Stachel T, Harris JW (2003) Li abundances in inclusions in diamonds
524 from the upper and lower mantle. Chem Geol 201:307-318
525 Seitz H-M, Brey GP, Zipfel J, Ott U, Weyer S, Durali S, Weinbruch S (2007) Lithium isotope
526 composition of ordinary and carbonaceous chondrites, and differentiated planetary
527 bodies: Bulk solar system and solar reservoirs. Earth Planet Sc Lett 260:582–596
528 Seitz H-M, Woodland AB (2000) The distribution of lithium in perodotite and pyroxenitic
529 mantle lithologies - an indicator of magmatic and metasomatic processes. Chem Geol
530 166:47-64
531 Stachel T, Harris JW, Brey GP, Joswig W (2000) Kanakan diamonds (Guinea) II: lower
532 mantle inclusion parageneses. Contrib Mineral Petr 140:16-27
533 Stachel T, Harris JW, Aulbach S, Deines P (2002) Kankan diamonds (Guinea) III: $\delta^{13}C$ and
534 nitrogen characteristics of deep diamonds. Contrib Mineral Petr 142:465–475

Stachel T, Harris JW, Muehlenbachs K (2009) Sources of carbon in inclusion bearing diamonds. Lithos 112S:625-637

Taylor WR, Green DH (1987) The petrogenetic role of methane: Effect on liquidus phase relations and the solubility mechanism of reduced C-H volatiles. In: Mysen BO (ed) Magmatic processes: Physicochemical principles. The Geochemical Society, London, pp. 121-138, Spec. Publ. No. 1

Thomson AR, Kohn SC, Bulanova GP, Smith CB, Araujo D, Walter MJ (2014) Origin of sub-lithospheric diamonds from the Juina-5 kimberlite (Brazil): constraints from carbon isotopes and inclusion compositions. Contrib Mineral Petr 168:1081-1088

Thomson AR, Kohn SC, Bulanova GP, Smith CB, Araujo D, Walter MJ (2016) Trace element composition of silicate inclusions in sub-lithospheric diamonds from the Juina-5 kimberlite: evidence for diamond growth from slab melts. Lithos 265:108–124

Tomascak PB (2004) Developments in the understanding and application of lithium isotopes in the Earth and Planetary sciences. In: Johnson C, Beard B, Albarède F (eds) Geochemistry of non-traditional stable isotopes. Rev Mineral Geochem, vol 55. Miner Soc Am, Washington DC, pp 153-195

Tomascak PB, Langmuir CH (1999) Lithium isotope variability in MORB. EOS 80, F1086-F1087

Van Orman J, Grove TL, Shimizu N (2001) Rare earth element diffusion in diopside: influence of temperature, pressure, and ionic radius, and an elastic model for diffusion in silicates. Contrib Mineral Petr 141:687-703

Vils F, Tonarini S, Kalt A, Seitz H-M (2009) Boron, Lithium and strontium isotopes as tracers of seawater-serpentinite interaction at Mid-Atlantic Ridge, ODP Leg 209. Earth Planet Sc Lett 286:414-425

559 Walter MJ, Bulanova GP, Armstrong LS, Keshav S, Blundy JD, Gudfinnsson G, Lord OT,
560 Lennie AR, Clark SM, Smith CB, Gobbo L (2008) Primary carbonatite melt from
561 deeply subducted oceanic crust. Nature 454:622-625
562 Walter MJ, Kohn SC, Araujo D, Bulanova GP, Smith CB, Gaillou E, Wang J, Steele A,
563 Shirey SB (2011) Deep Mantle Cycling of Oceanic Crust: Evidence from Diamonds
564 and Their Mineral Inclusions. Science 334:54-57
565 Wilding MC (1990) A study of diamonds with syngenetic inclusions. PhD Thesis. University
566 of Edinburgh, UK
567 Wirth R, Kaminsky F, Matsyuk S, Schreiber A (2009) Unusual micro- and nano-inclusions in
568 diamonds from Juina Area, Brazil. Earth Planet Sc Lett 286:292-303
569 Wirth R, Dobrzhinetskaya L, Harte B, Schreiber A, Green H.W. (2014) High-Fe (Mg,Fe)O
570 inclusion in diamond apparently from the lowermost mantle. Earth Planet Sc Lett
571 404:365-375
572 Wunder B, Deschamps F, Watenphul A, Guillot S, Meixner A, Romer RL, Wirth R (2010)
573 The effect of chrysotile nanotubes on the serpentine-fluid Li-isotopic fractionation.
574 Contrib Mineral Petr 159:781–790
575 Yacob JL, Feinemann MD, Deane Jr. JA, Eggler DH, Penniston-Dorland SC (2012) Lithium
576 partitioning between olivine and diopside at upper mantle conditions: An experimental
577 study. Earth Planet Sc Lett 329-330:11-21
578 Zack T, Tomascak, PB, Rudnick RL, Dalpe C, McDonough WF, (2003) Extremely light Li in
579 orogenic eclogites: The role of isotope fractionation during dehydration in subducted
580 oceanic crust. Earth Planet Sc Lett 208:279-290
581 Zedgenizov, D. A., Kagi, H., Shatsky, V. S. & Ragozin, A. L. 2014. Local variations of
582 carbon isotope composition in diamonds from São Luiz (Brazil): evidence for
583 heterogenous carbon reservoir in sublithospheric mantle. Chem Geol 363:114–124

584 **Figure captions**

585

586 **Fig. 1** Range of composition of ferropericlase, olivine (presumably former ringwoodite) and
587 MgSi-perovskite inclusions in ultradeep diamonds from Sao Luiz (Juina). (Harte, 2010; Harte
588 et al., 1999; Hayman et al., 2005; Hutchinson et al., 2001; Kaminsky et al., 2001; Wilding,
589 1990; Wirth et al., 2009). Pairrs of ringwoodite and ferropericlase from single diamonds are
590 connected by tie-lines

591

592 **Fig. 2a-d** Li, NiO, MnO and Na_2O abundances in ferropericlase inclusions as a function of
593 Mg# (Mg/(Mg+Fe^{tot})* 100). PUM - Primitive Upper Mantle composition estimated from
594 Kankan fper inclusions of Stachel et al. (2000). Data source as for Fig. 1

595

596 **Fig. 3** Li abundances and Li isotope compositions in ferropericlases from Sao Luiz diamonds,
597 in comparison to the fields delineating the Li isotopic compositions and Li contents for
598 subduction related components based on data for eclogites (Marschall et al., 2007; Zack et al.,
599 2003), serpentinized peridotites (Benton et al., 2004; Decitre et al., 2002; Vils et al., 2009),
600 marine sediments (Bouman et al., 2004; Chan et al., 2006), fresh MORB (Tomascak, 2004;
601 Tomascak and Langmuir, 1999; Marschall et al., 2017), altered MORB (Bouman et al., 2004;
602 Chan et al., 2002; Chan et al., 1992) and Primitive Upper Mantle (Seitz et al., 2004; Seitz et
603 al., 2007; Seitz and Woodland, 2000)

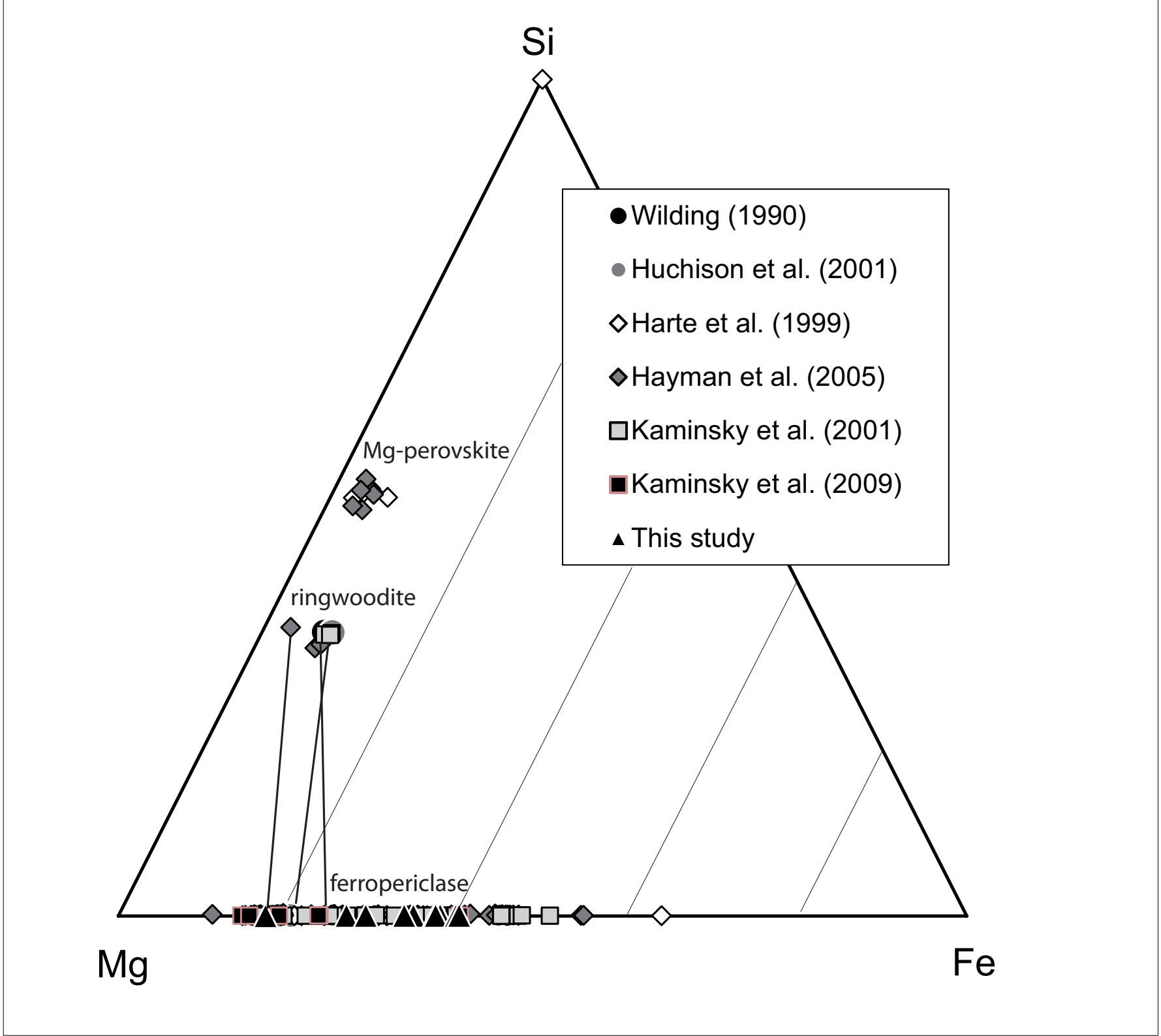

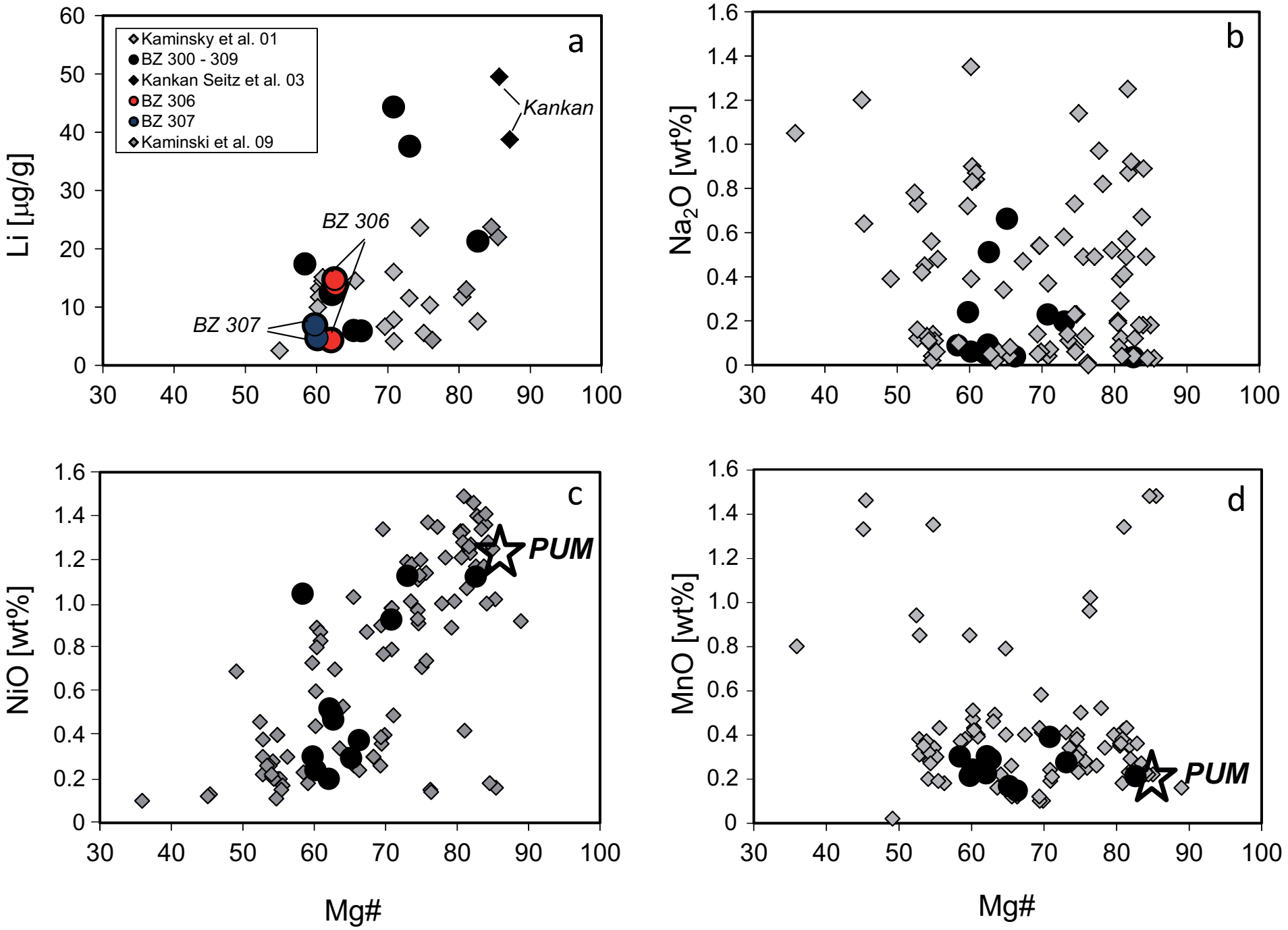

-

Colour Figure

Click here to download Colour Figure Figure 3.eps

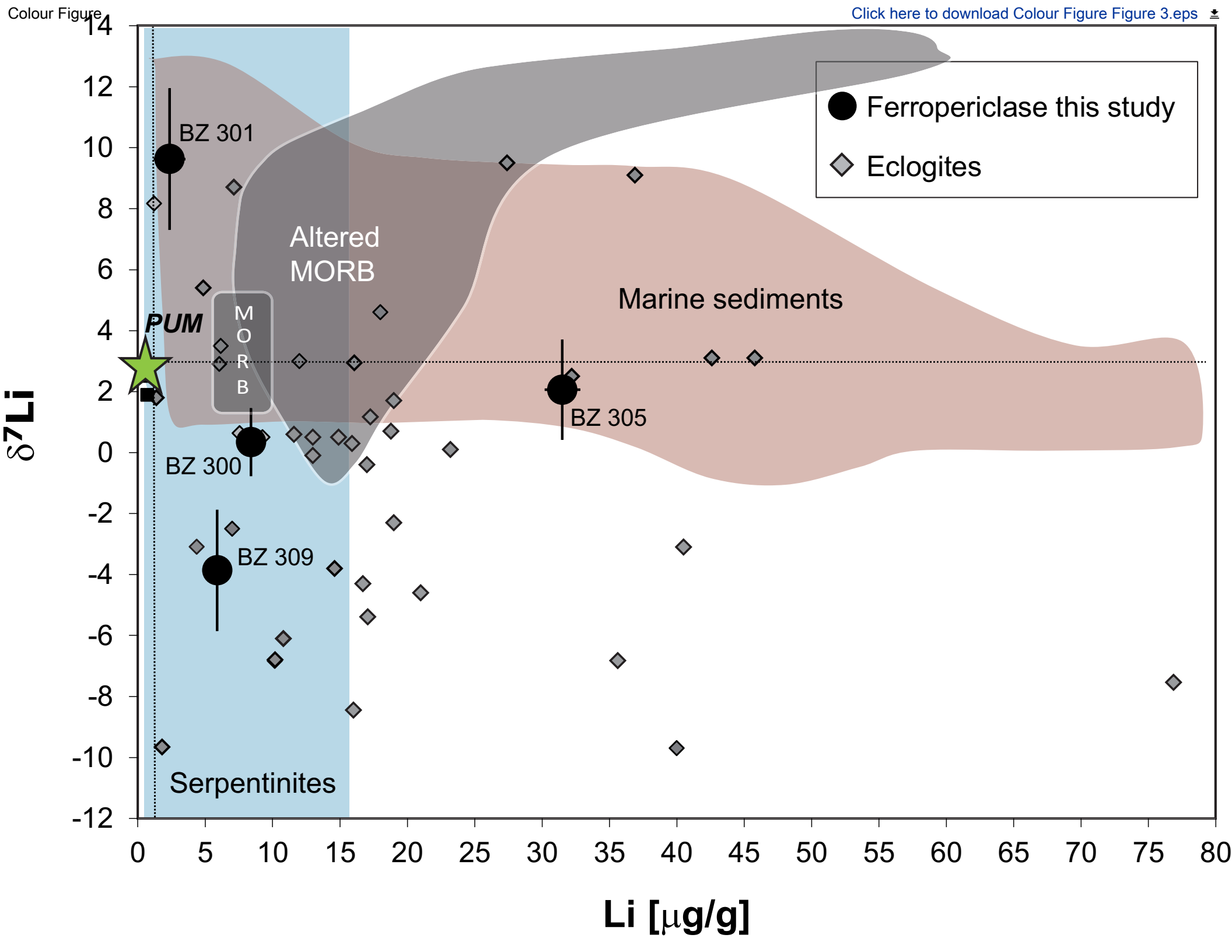

Table

Table 1

Lithium concentrations and isotopic compositions of ferropriclase inclusions in diamonds from Sao L

Sample	Inclusion	approx. size	Run	Li µg/g	2σ	δ^7Li	2σ
BZ 300	1	100*100*20		8.4	0.5		
	2, 3	>300*300*100	46	n.d.		0.5	1.1
BZ 301	2 to 8	80*80*20	52	2.4	1.4	9.6	1.2
BZ 302	1	200*150*150		37.6	0.4		
BZ 303	1	400*200*150		17.4	0.2		
BZ 304	1	250*150*100		6.0	0.1		
BZ 305	1	120*100*20		31.5	1.3		
	2, 3	>300*200*100	52	n.d.		2.1	0.7
BZ 306	2	100*100*20		13.9	0.1		
	3	200*100*50		4.3	0.2		
	4	200*100*100		14.7	0.1		
BZ 307	1	150*100*50		4.7	0.4		
	2	>200*200*100		6.8	0.1		
BZ 308	1	200*200*30		44.3	0.3		
BZ 309	1	150*100*80		5.9	0.2		
	2 to 5	>150*150*50	52	n.d.		-3.9	1.3

Corresponding to 'Run' numbers (analytical sessions) 'n' represents the number of measurements o
Uncertainty is the 2σ standard deviation. SIMS: secondary ion mass spectrometry, MC-ICPMS: mul
coupled plasma mass spetrometry. Not determined: n.d.

BZ300	ICP		300*300	300*300*250			
BZ301	ICP	**5 incl. +?**	500*200	200*200*100	200*1	200*80*20	150*
			150*20*	150*50*20	150*50*20		
BZ302	EPMA/SIMS		200*150*150				
BZ303	EPMA/SIMS		400*200*150				
BZ304	EPMA/SIMS		250*150*100				
BZ305	ICP		300*200	400*300*150			
BZ306	EPMA/SIMS		400*200	200*100*50	200*100*100		
BZ307	EPMA/SIMS		200*200*100				
BZ308	EPMA/SIMS		200*200	200*200*30			
BZ309	ICP	**2 incl. +?**	350*200	300*200*50	200*2	150*150*50	

EMPA

BZ300	EPMA/SIMS		100*100*20
BZ301		**lost**	80*80*20
BZ305	EPMA/SIMS		120*100*20
BZ306	EPMA/SIMS	**ilmenite**	100*100*20
BZ307	EPMA/SIMS		150*100*50
BZ309	EPMA/SIMS		150*100*80

.uiz

n	Method
	SIMS
4	MC-ICPMS
3	MC-ICPMS
	SIMS
	SIMS
	SIMS
	SIMS
3	MC-ICPMS
	SIMS
	SIMS
	SIMS
	SIMS
	SIMS
	SIMS
	SIMS
3	MC-ICPMS

n given solutions.
ti collector iductively

100*50

Table 1
Lithium concentrations and isotopic compositions of ferropericlase inclusions in diamonds from Sao Luiz

Sample	Inclusion	approx. size in μm	Li μg/g	2σ	δ^7Li	2σ	n	Method
BZ 300	1	100*100*20	8.4	0.5				SIMS
	2, 3	>300*300*100	n.d.		0.5	1.1	4	MC-ICPMS
BZ 301	2 to 8	80*80*20	2.4	1.4	9.6	1.2	3	MC-ICPMS
BZ 302	1	200*150*150	37.6	0.4				SIMS
BZ 303	1	400*200*150	17.4	0.2				SIMS
BZ 304	1	250*150*100	6.0	0.1				SIMS
BZ 305	1	120*100*20	31.5	1.3				SIMS
	2, 3	>300*200*100	n.d.		2.1	0.7	3	MC-ICPMS
BZ 306	2	100*100*20	13.9	0.1				SIMS
	3	200*100*50	4.3	0.2				SIMS
	4	200*100*100	14.7	0.1				SIMS
BZ 307	1	150*100*50	4.7	0.4				SIMS
	2	>200*200*100	6.8	0.1				SIMS
BZ 308	1	200*200*30	44.3	0.3				SIMS
BZ 309	1	150*100*80	5.9	0.2				SIMS
	2 to 5	>150*150*50	n.d.		-3.9	1.3	3	MC-ICPMS

Corresponding to 'Run' numbers (analytical sessions) 'n' represents the number of measurements on given solutions. Uncertainty is the 2σ standard deviation. SIMS: secondary ion mass spectrometry, MC-ICPMS: multi collector iductively coupled plasma mass spetrometry. Not determined: n.d.

Electronic Supplementary Material accompanying the article

"Ferropericlase inclusions in ultradeep diamonds from Sao Luiz (Brazil): High Li abundances and diverse Li-isotope and trace element compositions suggest an origin from a subduction mélange"

Hans-Michael Seitz • Gerhard P. Brey • Jeffrey W. Harris • Soodabeh Durali-Müller • Thomas Ludwig • Heidi E. Höfer

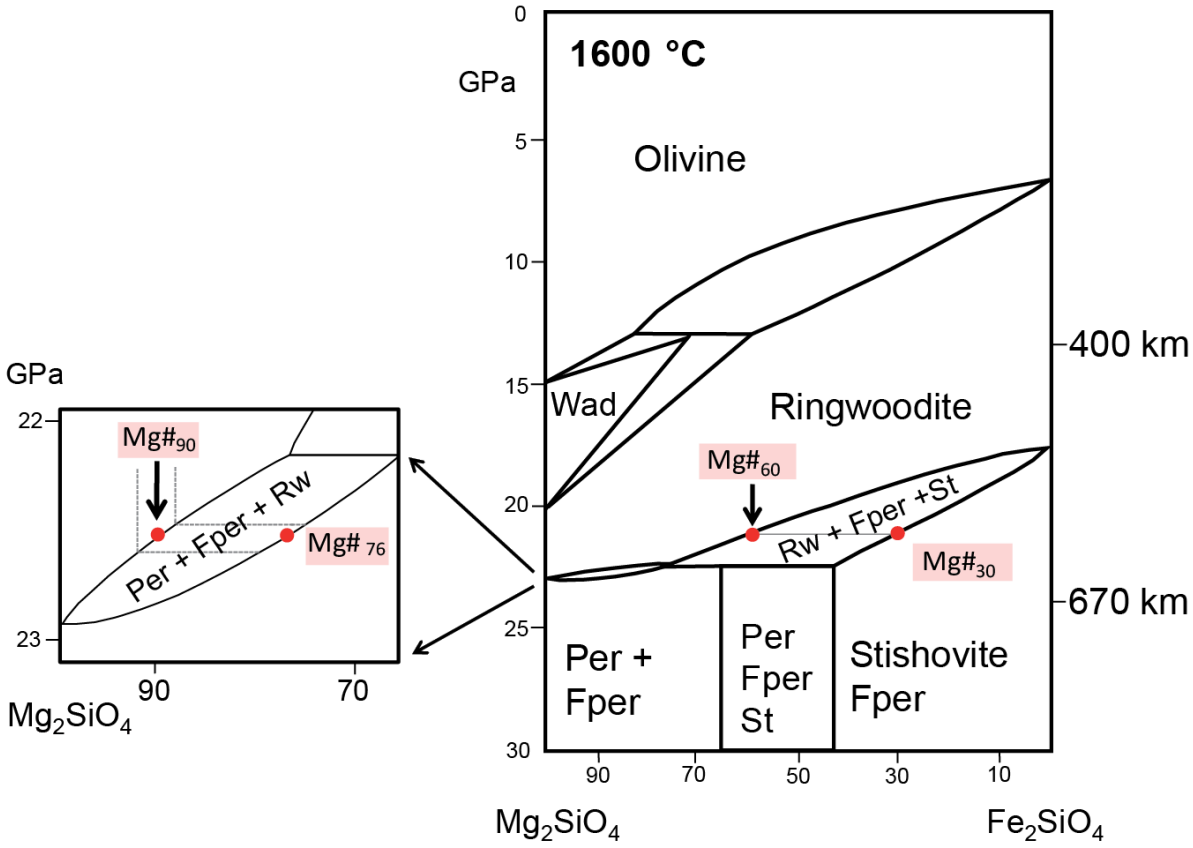

Fig. S1: Schematic phase diagram for the system forsterite – fayalite at constant temperature with phase changes occurring with increasing pressure. The Mg# of coesting ringwoodite and ferropericlase are calculated according to (Frost and Langenhorst, 2002; Frost et al., 2001) and given as Mg# for selected examples.

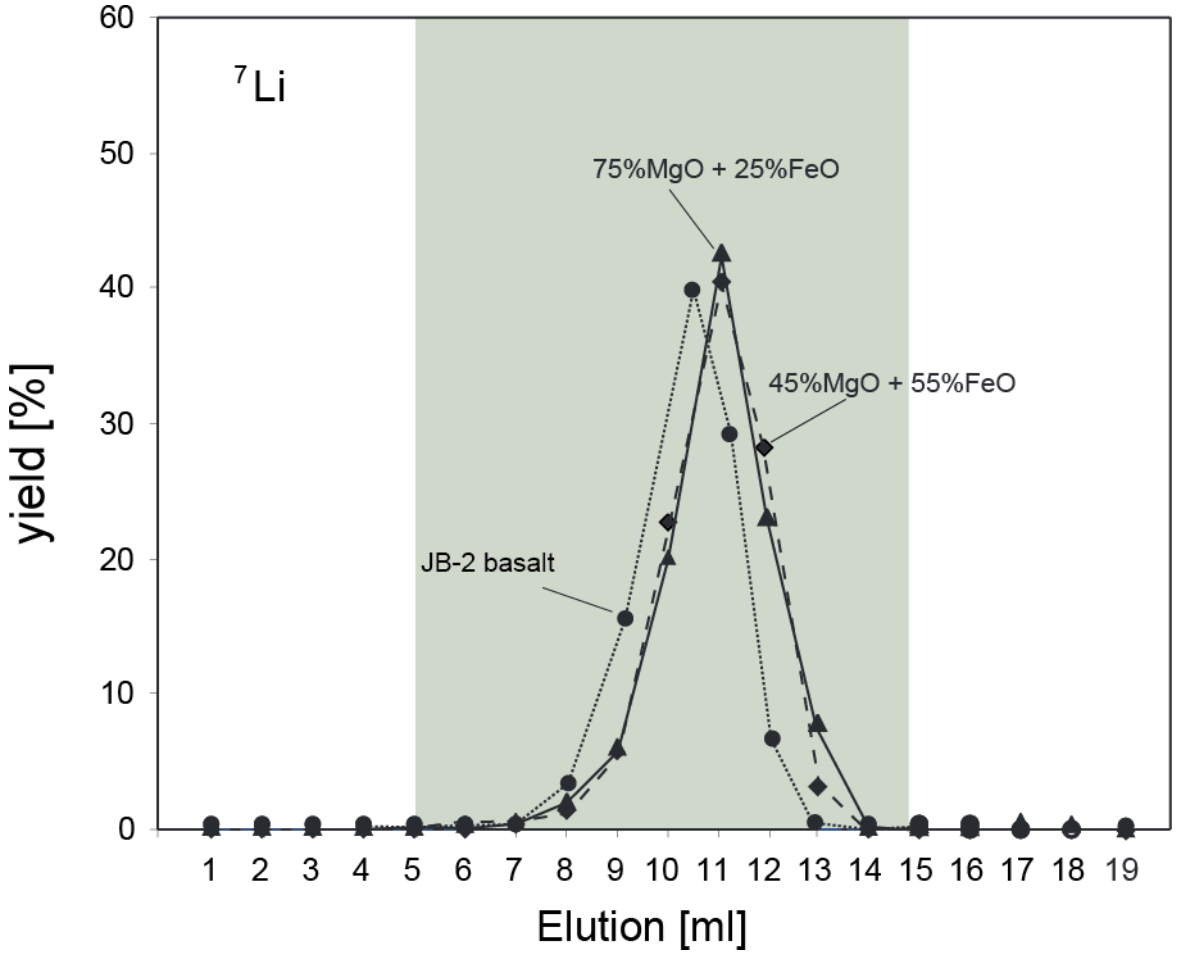

Fig. S2: Elution-curves of two ferropericlase solutions (45 wt% MgO/55 wt% FeO and 75 wt% MgO/25% FeO) in comparison to the basalt standard JB-2 using a 1.4 ml column and AG 50W-X8 resin. A 10 ml fraction (shaded area) was collected for quantitative recovery of Li.

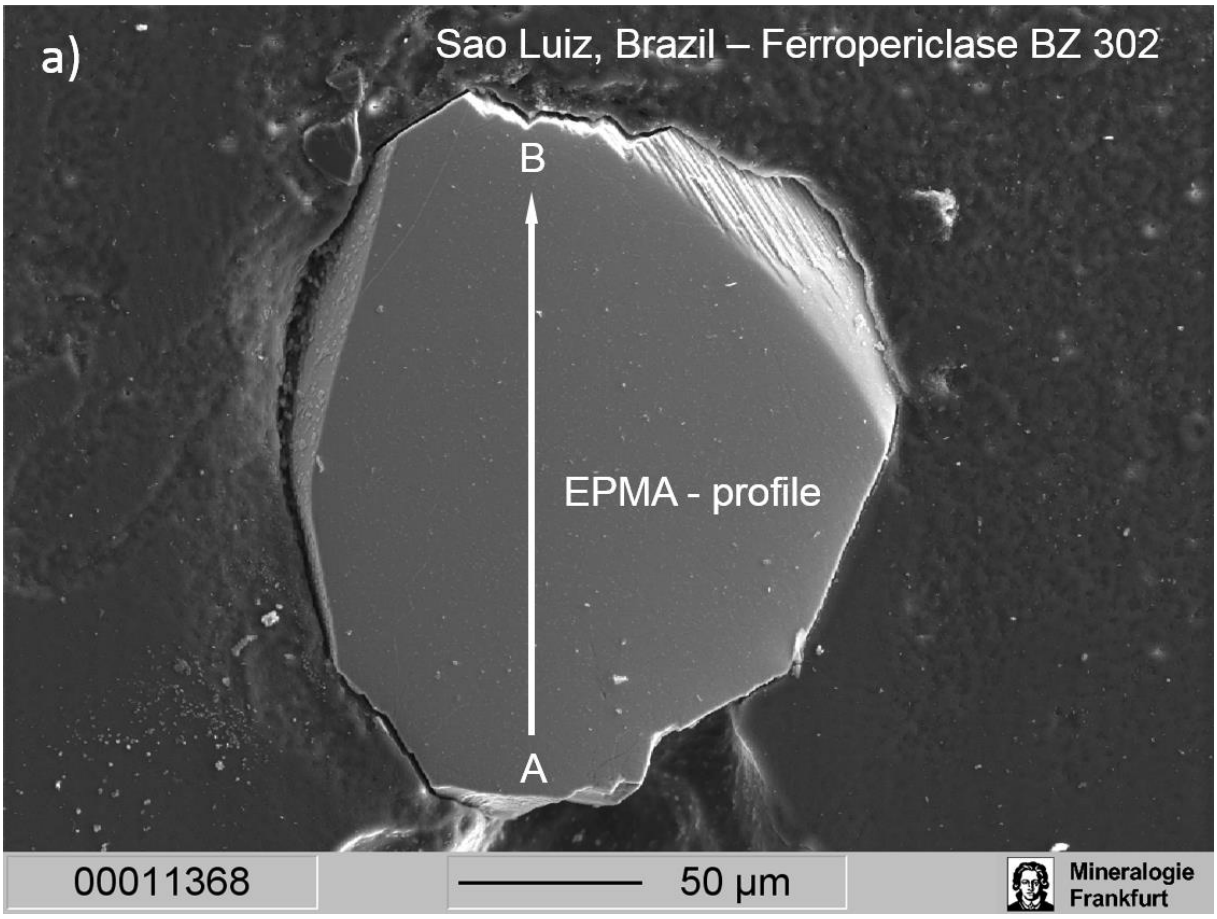

Fig. S3: a) Combined backscattered and secondary electron image of ferropericlase in diamond BZ302.

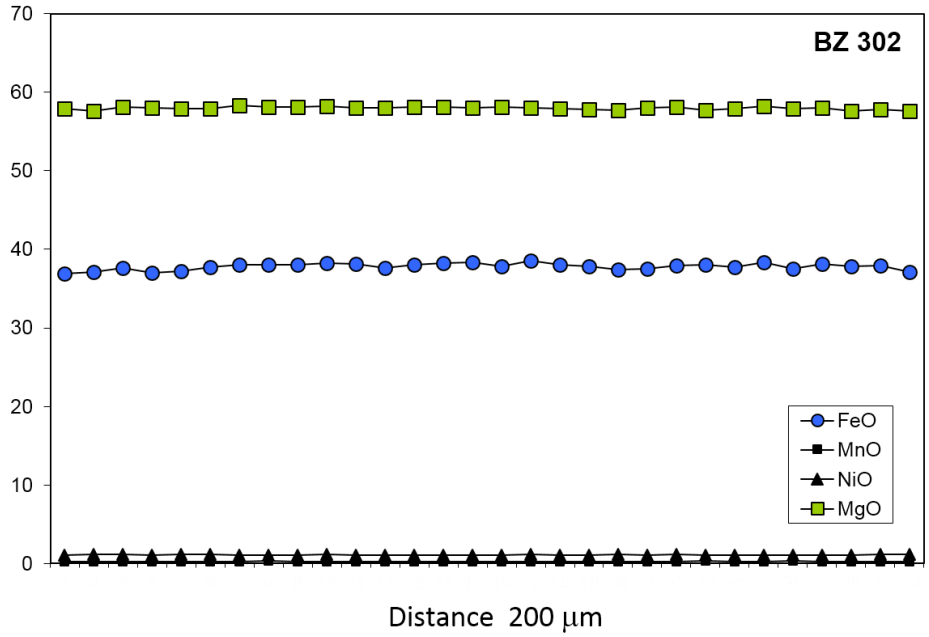

Figure 3b appendix: Seitz et al.

Fig. S3: b) Element profile obtained by electron microprobe analysis (EPMA)

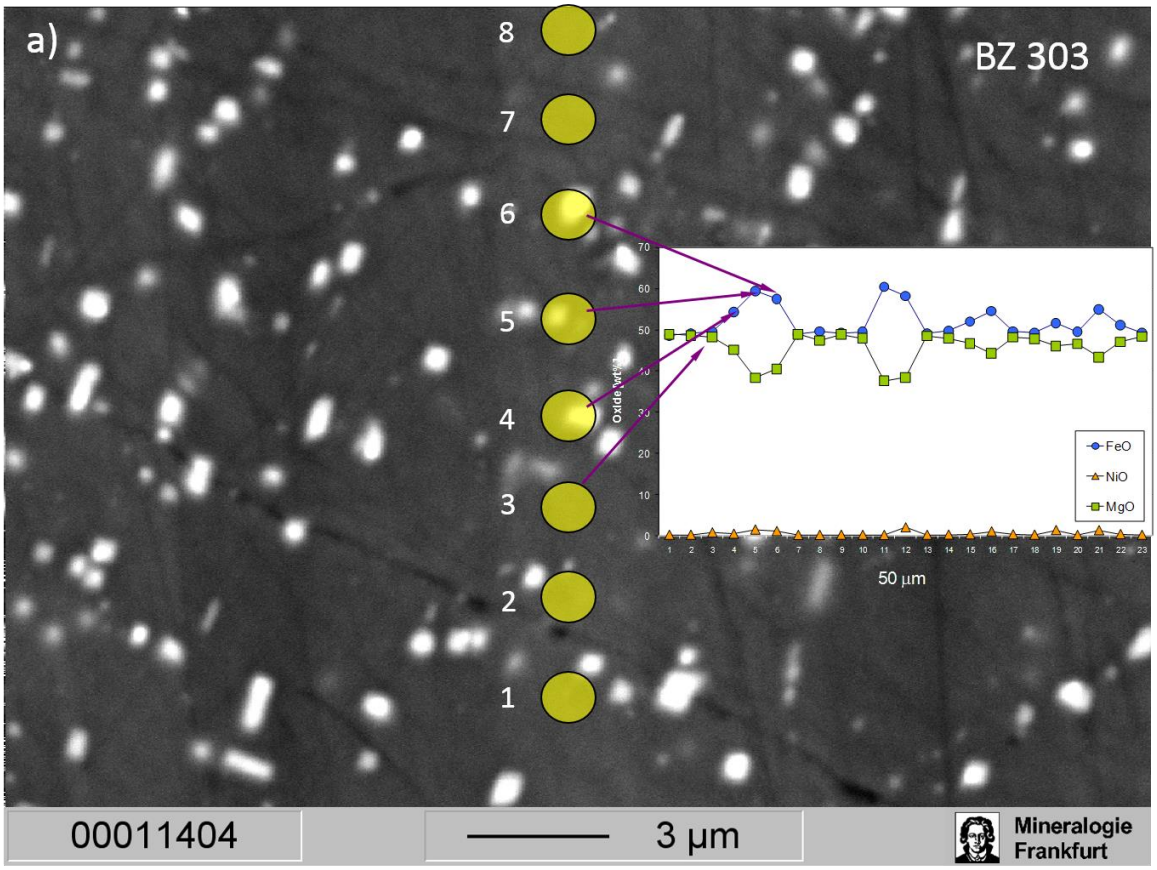

Figure 4a appendix: Seitz et al.

Fig. 4: a) Element profile and back scattered image (BSE) of magnesioferrite exsolutions in ferropericlase BZ 303. The numbered yellow dots give the approximate position of the focused electron beam. The bright « spots » are the magnesioferrite inclusions. Fe and Ni increase where the beam diameter overlaps with these bright spots.

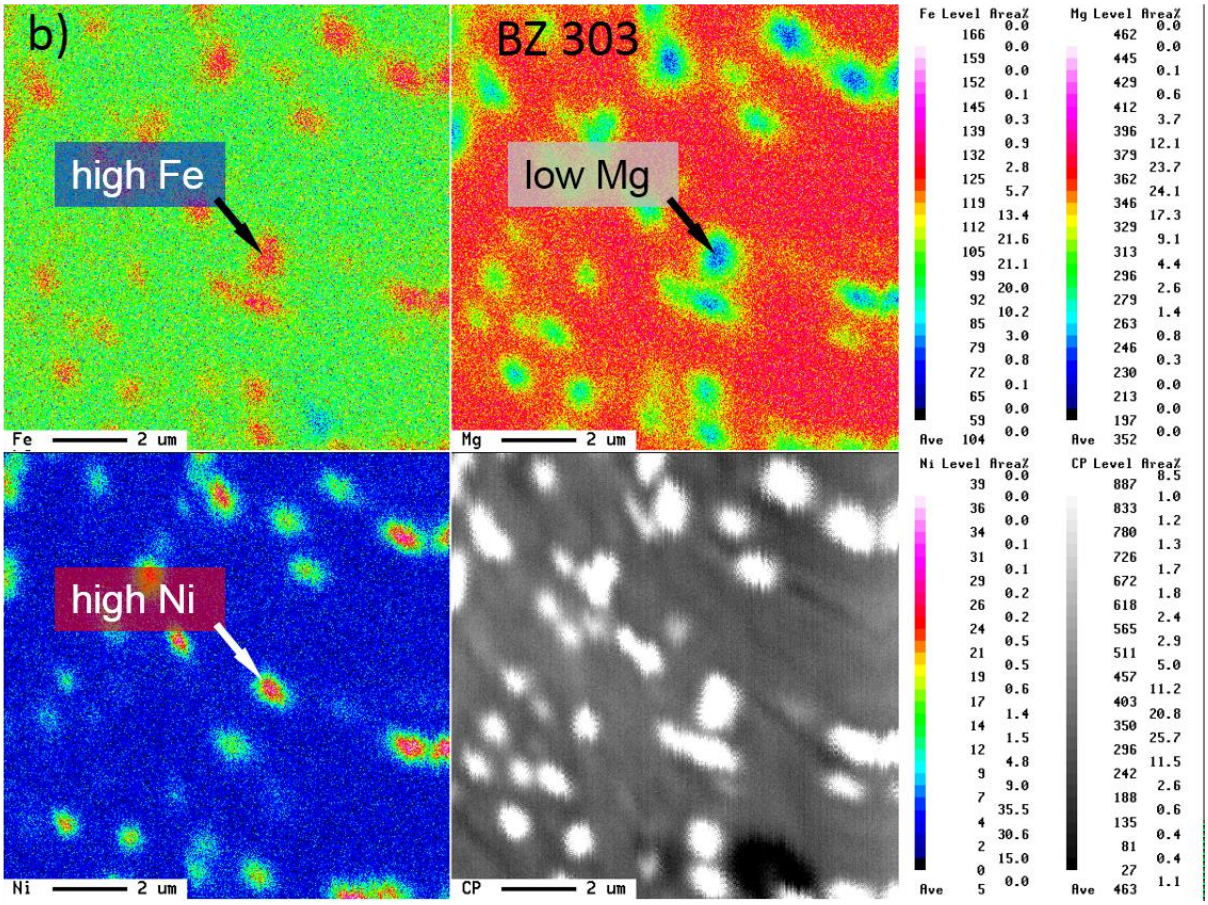

Fig. S4: b) An energy-dispersive X-ray map of magnesioferrite exsolutions